

Computer Simulation of Purkinje Fibres from a Rabbit Model of Congestive Heart Failure

Jue Li, Sunil Jit Logantha, Joseph Yanni, Xue Cai, Henggui Zhang, Halina Dobrzynski, George Hart, Mark Boyett

Institute of Cardiovascular Sciences, University of Manchester, United Kingdom

Abstract

This study used computer simulation to investigate the influence of heart failure (HF) on the Purkinje fibre. The study was based on a rabbit model of HF caused by volume and pressure overload. In the left ventricular free running Purkinje fibres, the expression level of the key cardiac ion channels was measured at the mRNA (messenger RNA) level using qPCR (quantitative polymerase chain reaction). Major changes were observed. To simulate the effect of these changes, we began with a model of the healthy rabbit Purkinje fibre action potential. In the absence of ionic current measurements from failing rabbit Purkinje fibres, we assumed that changes in ionic currents mirrored changes in ion channel expression: ionic conductances were adjusted based on changes in expression of the relevant ion channels. In the simulations, if all changes observed were incorporated, the Purkinje fibre is predicted to become inexcitable. Such an outcome would result in left bundle branch block (as observed in HF patients). The simulations predict that HF-dependent changes in I_{NaL} , I_{to} , I_{Kr} and I_{K1} and will have the most influence on the Purkinje fibre action potential. The predicted changes in the Purkinje fibre action potential were compared to actual changes measured using sharp microelectrodes.

1. Introduction

The His-Purkinje network conducts the action potential from the atrioventricular node to the ventricles and causes them to contract. However, it is also believed to play important roles in the generation of ventricular arrhythmias, particularly those related to triggered activity. Heart failure (HF) causes dysfunction of the network. For example, ~25% of HF patients have left bundle branch block [1].

The action potential is generated by voltage-gated ion channels embedded in a cell's plasma membrane. Ion channels are pore-forming membrane proteins whose functions include establishing a resting membrane potential, shaping action potentials and other electrical

signals by gating the flow of ions across the cell membrane.

Techniques for studying ion channels include patch clamp (measures ionic currents through ion channels), immunohistochemistry (measures ion channel proteins) and qPCR (measures ion channel mRNAs). Computer simulation is a useful tool to understand the physiology and pathophysiology of cardiac tissues. Many action potential models have been developed based on ionic currents measured using patch clamp. However, ionic current measurements from rabbit Purkinje fibres that have been modified by heart failure are not available.

This study was based on a rabbit model of congestive HF. The expression level of the key cardiac ion channels was measured at the mRNA level. The changes in ionic currents caused by HF were assumed to mirror changes in ion channel expression. A model of the healthy rabbit Purkinje fibre action potential was used [2]. According to the assumption above, the ionic conductances in the model were adjusted based on the changes in expression of the relevant ion channels (at the mRNA level), to predict the changes in the Purkinje fibre action potential caused by HF. The predicted changes in the Purkinje fibre action potential were compared to actual changes measured using sharp microelectrodes.

2. Methods

A rabbit model of left ventricular HF caused by volume and pressure overload was used. In the left ventricular free running Purkinje fibres, the expression level of the key cardiac ion channels was measured at the mRNA level using qPCR. Major changes were observed: for example, in HF, $Na_v1.1$ and $Na_v1.5$ (responsible for I_{Na} and I_{NaL}) were downregulated by 87% and 59%, $Ca_v1.2$ and $Ca_v1.3$ (responsible for I_{CaL}) were downregulated by 62% and 90%, $K_v4.2$ (responsible for I_{to}) was downregulated by 96%, $K_v4.3$ (also responsible for I_{to}) was upregulated by 18%, $K_v1.5$ (responsible for I_{Kp}) was downregulated by 81%, hERG (responsible for I_{Kr}) was downregulated by 64%, $KvLQT1$ and $minK$ (responsible for I_{Ks}) were downregulated by 89% and

55%, $K_{ir2.1}$ and $K_{ir2.2}$ (responsible for I_{K1}) were downregulated by 79% and 97%, the Na^+-K^+ pump (responsible for I_{NaK}) was downregulated by 40%, NCX1 (responsible for I_{NaCa}) was downregulated by 54%, RYR2 (responsible for sarcoplasmic reticulum - SR - Ca^{2+} release) was downregulated by 22% and SERCA2 (responsible for SR Ca^{2+} uptake) was downregulated by 34%.

To simulate the effects of the HF-induced changes in ion channels on Purkinje fibre action potentials, a model of the healthy rabbit Purkinje fibre action potential [2] was used. General equations are:

$$\frac{dV}{dt} = -\frac{I_{ion}}{C_m} \quad (1)$$

$$I_{ion} = I_{Na} + I_{NaL} + I_{CaL} + I_{CaT} + I_{to} + I_{Kr} + I_{Ks} + I_{K1} + I_{Kp} + I_{NaCa} + I_{NaK} + I_{Na,b} + I_{Ca,b} + I_{K,b} + I_{Cl} + I_{Cl,b} + I_{SLCa,p} \quad (2)$$

Where V (mV) is the membrane potential, t (ms) is the time, I_{ion} (pA) is the total membrane current, and C_m (pF) is the membrane capacitance. The total membrane current includes seventeen components which are shown in equation (2).

HF-induced changes in ionic currents in rabbit Purkinje fibres have not been measured. We assumed that changes in ionic currents mirrored changes in ion channel expression. However, HF-induced changes in ionic currents and action potentials in canine cardiac Purkinje cells have been evaluated [3]. The results show that there were no differences in the form of the current-voltage relationships while the relevant currents densities were significantly smaller. Based on these results and our assumption above, the ionic conductances can be adjusted based on changes in expression of the relevant ion channels to simulate the Purkinje fibre action potential in HF.

In some cases, several ion channels are responsible for an ionic current. For example, both $K_{ir2.1}$ and $K_{ir2.2}$ are responsible for I_{K1} . To determine the changes in ionic conductances, ion channels are assumed to be arranged in parallel and not to interact. Then we have:

$$g'_{ion} = \frac{(\sum_{i=1}^n \gamma_{ion}^i d_{ion}^i)_{HF}}{(\sum_{i=1}^n \gamma_{ion}^i d_{ion}^i)_{control}} \times 100\% \quad (3)$$

Where g'_{ion} is the ratio between the ionic conductance in HF compared to the ionic conductance in control. d_{ion} is ion channel expression (or density). γ_{ion} is the single channel conductance. n is the total number of different

ion channel types which are responsible for one ionic current.

Table 1 shows the single channel conductance of ion channels which contribute to three important ionic currents (I_{to} , I_{Kr} and I_{K1}), ion channel expression (based on the ΔCt calculation) in the left ventricular free running Purkinje fibres from control and heart failure rabbits, and, finally, the HF:control ratio of ionic conductances calculated by equation (3).

Table 1. Single channel conductance, ion channel expression in the left ventricular free running Purkinje fibres from control and heart failure rabbits, and the HF:control ratio of ionic conductances

Ionic currents and channels	γ_{ion} (pS)	d_{ion} Control ($\times 10^{-6}$)	d_{ion} HF ($\times 10^{-6}$)	g'_{ion}
I_{to}				
$K_{v4.2}$	18.3 [4]	157.598	6.74575	
$K_{v4.3}$	4.0 [5]	5.86528	6.91767	5.2%
I_{Kr}				
ERG		2.81212	1.00131	35.6%
I_{K1}				
$K_{ir2.1}$	23.8 [6]	137.649	28.915	
$K_{ir2.2}$	34.0 [6]	82.4781	2.44286	12.7%

According to the changes in expression level of the key cardiac ion channels measured at the mRNA level using qPCR, ten ionic currents were remodelled to: I_{Na} , 34%; I_{NaL} , 34%; I_{CaL} , 21%; I_{to} , 5%; I_{Kp} , 19%; I_{Kr} , 36%; I_{Ks} , 11%; I_{K1} , 13%; I_{NaCa} , 46%; I_{NaK} , 60%. Apart from these ten ionic currents, Ca^{2+} uptake and release through the SR were remodelled to 66% and 78% based on the changes in expression level of SERCA2 and RYR2.

3. Results

3.1. Sensitivity of the Purkinje fibre action potential to ion channel remodelling

The influence of ion channel remodelling on the action potential in Purkinje fibres was investigated. Based on the qPCR data, in HF the mRNA level of most key ion channels was downregulated. To simulate the effects of downregulation of ionic currents on the Purkinje fibre action potential, every ionic current was studied separately. Each ionic conductance was reduced by 50%. Figure 1 shows that 50% reduction of I_{NaL} , I_{CaL} , I_{to} , I_{Kr} , I_{K1} , I_{NaK} and Ca^{2+} uptake has a substantial effect on Purkinje fibre action potential duration (APD) (changed by -26%, -9%, +7% +19%, +39%, +12% and +10%; measured at -80 mV). 50% reduction of I_{CaT} , $I_{Ca,b}$, I_{NaCa} and Ca^{2+} release has less influence on Purkinje fibre APD (changed by -3%, -4%, -4%, and -3%;

measured at -80 mV). Reduction of I_{Na} , I_{Kp} , I_{Ks} , I_{Cl} , $I_{SLCa,p}$, $I_{Na,b}$, $I_{K,b}$ and $I_{Cl,b}$ had no influence on Purkinje fibre APD. However, 50% reduction of I_{Na} reduced the maximum upstroke velocity by 43%. 50% reduction of I_{CaL} caused early afterdepolarization-like events (EADs) (Figure 2).

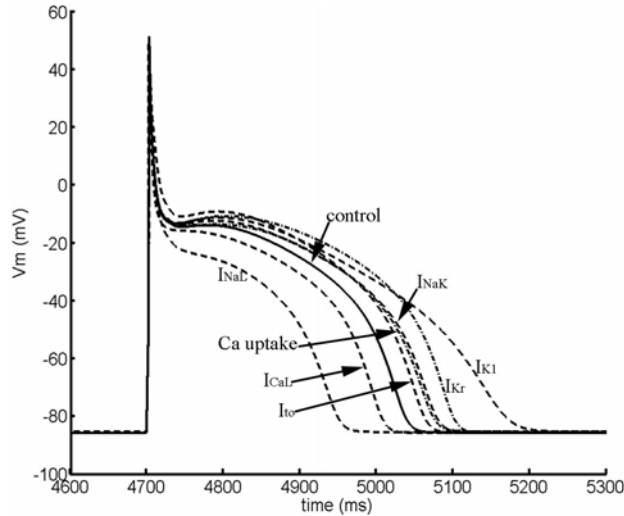


Figure 1 Simulation of effects of 50% reduction of I_{NaL} , I_{CaL} , I_{to} , I_{Kr} , I_{K1} , I_{NaK} and Ca^{2+} uptake on Purkinje fibre action potentials at 1000 ms cycle length.

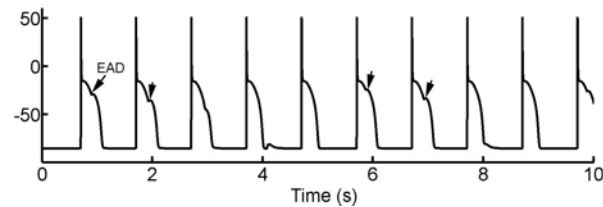


Figure 2 EAD-like events caused by 50% reduction of I_{CaL} at 1000 ms cycle length.

3.2. Influence of HF-induced ion channel remodelling on the Purkinje fibre action potential

The changes in ion channel expression (measured at the mRNA level using qPCR) were incorporated into the Purkinje fibre model by adjusting the ionic conductances of the relevant ionic currents.

Figure 3 shows the changes in the Purkinje fibre action potential at a cycle length of 3000 ms caused by adjusting the ionic conductances. The downregulation of I_{K1} had the most influence on the action potential (Figure 3C). The change prolonged the action potential more than three times, and caused EADs. Although the change in I_{to} was larger than the change in I_{Kr} , the change in I_{Kr} had more influence than the change in I_{to} on the APD (Figure 3A, B). However, the change in I_{to} had more influence than the change in I_{Kr} on the plateau of the

action potential (Figure 3A inset). The change in I_{NaL} reduced the APD (Figure 3A). The change in I_{CaL} also reduced APD (Figure 3B). Figure 3D shows the action potential after incorporation of all changes in HF (solid line), incorporation of the changes in $I_{NaL}+I_{to}+I_{Kr}+I_{K1}$ (dashed line) and the changes in $I_{NaL}+I_{CaL}+I_{to}+I_{Kr}+I_{K1}$ (dot-dash line). The Purkinje fibre was predicted to become depolarized (potentially inexcitable) in the first two cases. However in third case, the Purkinje fibres were predicted to be remain polarized (and therefore excitable), but potentially vulnerable to EADs and delayed afterdepolarizations (DADs).

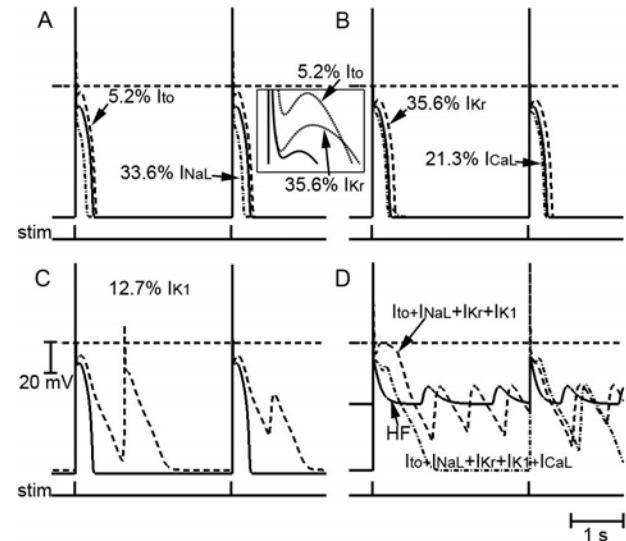


Figure 3 Simulation of effects of HF on the Purkinje fibre action potentials at 3000 ms cycle length. Action potential in control shown as a solid line in A-C. A: 33.6% I_{NaL} (dot-dash line) and 5.2% I_{to} (dashed line). B: 21.3% I_{CaL} (dot-dash line) and 35.6% I_{Kr} (dashed line). C: 12.7% I_{K1} (dashed line). D: all changes in HF incorporated (solid line), 33.6% I_{NaL} + 5.2% I_{to} + 35.6% I_{Kr} + 12.7% I_{K1} incorporated (dashed line) and 33.6% I_{NaL} + 21.3% I_{CaL} + 5.2% I_{to} + 35.6% I_{Kr} + 12.7% I_{K1} incorporated (dot-dash line).

3.3. Comparison between simulated and measured action potentials in HF

Action potentials in left free running Purkinje fibres were measured using sharp microelectrodes. One experimental result is shown in Figure 4C. Figure 4A shows two action potentials; the solid line shows the action potential after incorporating all changes in HF into the Purkinje fibre model; the dashed line shows the action potential after incorporating all changes, but assuming that the magnitude of the changes was 85% of that measured. This is equivalent to stating that the change in protein is less than the change in mRNA and this is not unreasonable (mRNA is translated to protein

and it is the protein that is responsible for function, i.e. ionic current in this case). Figure 4B shows the action potential after incorporating changes in five major ionic currents (33.6% I_{NaL} + 21.3% I_{CaL} + 5.2% I_{to} + 35.6% I_{Kr} + 12.7% I_{K1}). The results predict that: the Purkinje fibre becomes depolarized and inexcitable after incorporating all the changes in HF; the Purkinje fibre remains polarized and excitable, but exhibits EADs and DADs, after either scaling down the changes in HF or incorporating the changes in five major ionic currents only.

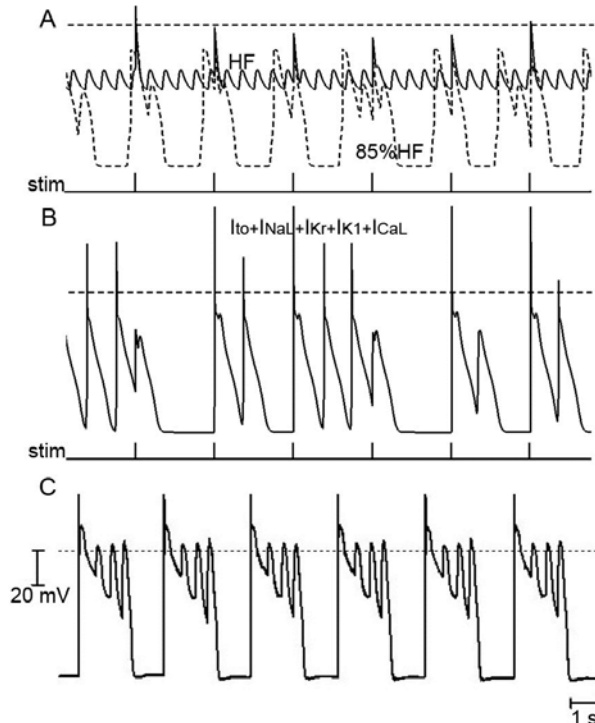


Figure 4 Purkinje fibre action potentials in HF at 3000 ms cycle length. A: simulation results from incorporation of all changes in HF (solid line) and incorporation of all changes, but assuming that the magnitude of the changes was 85% of that measured (dashed line). B: simulation result from incorporation of the HF-induced changes in five major ionic currents only (33.6% I_{NaL} + 21.3% I_{CaL} + 5.2% I_{to} + 35.6% I_{Kr} + 12.7% I_{K1}). C: action potentials recorded from the left free running Purkinje fibres from a HF rabbit.

4. Discussion

In this work, computer simulation was used to investigate the influence of HF on the Purkinje fibre. The results suggest:

1. The action potential is most sensitive to I_{K1} of the outward K^+ currents. The action potential is most sensitive to I_{NaL} of the inward ionic currents (Figure 1).

2. Downregulation of I_{CaL} may predispose to EAD-mediated arrhythmias (Figure 2).
3. Overall, the prolongation of the action potential caused by downregulation of outward currents is greater than the shortening caused by downregulation of inward currents (Figure 1).
4. Incorporation of all changes observed in HF into the Purkinje fibre model causes depolarization and inexcitability (Figure 4A). Many HF patients have left bundle branch and this may be the result of a similar loss of excitability.
5. Incorporation of all changes observed in HF, but assuming that the magnitude of the changes was 85% of that measured, caused EADs and DADs, but the Purkinje fibre remained excitable (Figure 4A). This is similar to the experimentally recorded case (Figure 4C). A similar result was obtained if the HF-induced changes in five major ionic currents only were incorporated (Figure 4B). EADs and DADs in HF could be responsible for ventricular tachyarrhythmias.

Acknowledgements

This work is supported by the British Heart Foundation (programme grant, RG/11/18/29257).

References

- [1] Baldasseroni S, et al. Left bundle-branch block is associated with increased 1-year sudden and total mortality rate in 5517 outpatients with congestive heart failure: A report from the Italian network on congestive heart failure. *Am Heart J* 2002;143:398-405.
- [2] Aslanidi OV, et al. Ionic mechanisms for electrical heterogeneity between rabbit Purkinje fiber and ventricular cells. *Biophys J* 2010;98:2420-31.
- [3] Han W, et al. Ionic Remodeling of cardiac Purkinje cells by congestive heart failure. *Circulation* 2001;104:2095-100.
- [4] Wang Z, et al. Increased focal Kv4.2 channel expression at the plasma membrane is the result of actin depolymerization. *Am J Physiol Heart Circ Physiol* 2004;286:H749-759.
- [5] Jerng HH, Qian Y, Pfaffinger PJ. Modulation of Kv4.2 channel expression and gating by dipeptidyl peptidase 10 (DPP10). *Biophys J* 2004;87:2380-2396.
- [6] Liu GX, et al. Comparison of cloned Kir2 channels with native inward rectifier K^+ channels from guinea-pig cardiomyocytes. *J Physiol* 2001;532:115-126.

Address for correspondence.

Dr. Jue Li

Full postal address: Cardiovascular Sciences Institute, University of Manchester, CTF Building, 46 Grafton Street, Manchester M13 9NT, UK
jue.li@manchester.ac.uk